Proceedings of the IASS 2024 Symposium
Redefining the Art of Structural Design
August 26-30, 2024, Zurich Switzerland
Philippe Block, Giulia Boller, Catherine DeWolf,
Jacqueline Pauli, Walter Kaufmann (eds.)

Enhancing mycelium-based composites: anisotropic material design and mechanical performance

Dana SAEZ*, Gianna HOFMAN, Denis GRIZMANN, Anett WERNER[a], Martin TRAUTZ

*Chair of Structures and Structural Design (Trako), Faculty of Architecture, RWTH Aachen University
Schinkelstr. 1, 52066, Aachen, Germany
saez@trako.arch.rwth-aachen.de

[a] AG Enzymtechnik, Chair of Bioprocess Engineering, Institute of Natural Materials Engineering,
Faculty of Mechanical Engineering, Dresden University of Technology

Abstract

Mycelium-based composites (MBC) emerge as a promising regenerative alternative for sustainable construction practices, harnessing rapid growth, resource efficiency, adaptability, biodegradability, carbon sequestration, and low energy requirements. These composite materials utilize fungal mycelium, forming a customizable matrix on a lignocellulosic base. The material's flexibility appeals to architects seeking innovative alternatives to traditional building materials, necessitating a deeper understanding of its mechanical properties for further improvements.

Prior optimizations of MBC relied on an isotropic approach, neglecting the potential advantages of anisotropic design through interface lamination. This research investigates anisotropic behavior in MBC with binding interfaces, evaluating their impact on load-bearing elements constructed from multiple mycelium composite base units. By combining mycelium and woody substrates, the study explores directional dependencies induced by the binding interfaces, presenting three engineered cases of anisotropy compared to standard isotropic test specimens.

The extended growth period required for a robust mycelial network poses a challenge, delaying experiments by up to two months. To overcome this, a non-linear Finite Element Method (FEM) is proposed for theoretical modeling, predicting variations worth investigating and saving time. The FEM simulations are validated through empirical tests, enabling controlled analysis of key variables like compression, bending, and shear forces.

Results indicate positive effects of mycelium binding interfaces on mechanical properties, particularly in compression and shear strengths. Moreover, this research underscores practical opportunities for improving material design processes. It highlights the ongoing evolution of mycelium-based materials in construction, contributing to the broader goal of sustainable and efficient building practices.

Keywords: mycelium-based composites, regenerative design, rapid growth, material design, mechanical properties, anisotropic design, sustainable construction practices, innovation in construction materials.

1. Introduction

With the recent emphasis on achieving carbon neutrality, particularly evident in proposals by the European Union, there is a pressing need to explore alternatives to materials with significant CO2 footprints [1]. MBC have emerged as a promising pathway for sustainable construction practices, leveraging their rapid growth, resource efficiency, adaptability, biodegradability, carbon sequestration

capabilities, and low energy requirements. These composite materials utilize fungal mycelium, forming a customizable matrix on a lignocellulosic base [2], [3]. Our research team focuses on optimizing MBC, which holds the potential to supplant several existing load-bearing components.

A precise understanding of a material's mechanical properties is essential for enhancing its performance. The optimization of load-bearing capacity in MBC has driven significant progress in their potential application in structural building elements. Although MBC present an anisotropic material structure, our research investigates how, through an aligned matrix achieved through binding-specific manufacturing conditions, it is possible to introduce a potentially favorable anisotropy into the composite material [4], [5].

The fungus requires extended growth periods to achieve a sufficiently vast mycelial network for creating robust solid material. This condition can delay experimental results by up to two months. In the initial developmental stage, we employ an accurate numerical model to simulate experiments, allowing for predictions of worthwhile variations to investigate. This approach saves time and adds scientific value. Subsequently, empirical tests are conducted based on the analyzed results of the numerical model.

Through FEM non-linear simulation of MBC, consisting of mycelium composite base units and pure mycelium binding layers, the effect of the pure mycelium layering is investigated. This data provides insights into the directional dependence of the composite material's mechanical properties.

We analyzed all simulated composites through compression, three-point bending, and shear tests, comparing results to data from previously tested MBC. Each case was tested with a minimum sample size of three. Compression tests were simulated with the material modeled cylindrically to ensure comparability with prior tests, while bending and shear experiments were simulated on cuboid-shaped materials. Subsequently, test specimens for empirical tests were manufactured accordingly.

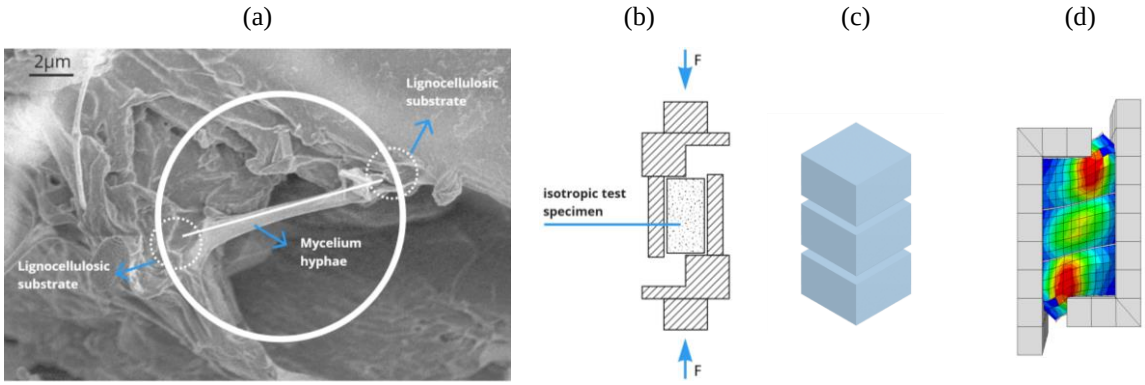

Figure 1: (a) mycelium binding capacity, (b) model for shear tests, (c) scheme of the test specimens with two binding interfaces, and (d) FEM shear simulation

1.2 Notes on the MBC composition

The MBC investigated in this paper is the result of research endeavors conducted at the Chair for Structures and Structural Design (TRAKO) at the RWTH Aachen in collaboration with the Institute of Natural Materials Engineering (INT) at the Technical University of Dresden during the research project MycoMatrix. It comprises *Ganoderma Lucidum* (GL) strain cultivated in a beech wood matrix. This composition was refined by varying matrix density, cultivation time, and conditions to enhance mechanical strength, aiming for optimal material strength for load-bearing element production using MBC. Consequently, all experiments in this study were explicitly conducted with this strain-lignocellulosic material composition. Nevertheless, the experimental approach and results can be extrapolated to a wide range of MBC compositions with minimal adjustments [6], [7], [8].

2. Methodology

Since the research of MBC focuses on the replacement of materials that are already in the market, when new materials are developed, it is crucial to characterize their properties to be compared to other existing

materials. Most material tests are destructive, meaning the sample will be deemed unusable after the test has commenced. The tests are designed to cause the material to fail so that its strength, stiffness, ductility, and failure mechanisms can be measured and analyzed. These tests are commonly used to evaluate materials' performance under different loading and environmental conditions to fulfill the construction standards.

A series of standard mechanical tests were conducted to comprehensively evaluate the developed material's mechanical properties (MBC). These tests included compression, three-point bending, and shear tests. Each test was performed following relevant European standards (DIN EN) to ensure consistency and reliability of results.

Compression tests were carried out to assess the material's response to compressive forces, providing insights into its compressive strength and deformation behavior under such loading conditions. Three-point bending tests were employed to evaluate the flexural properties of the material, including its modulus of elasticity and flexural strength. Additionally, shear tests were conducted to examine the material's shear strength and behavior under shear loading.

However, it is essential to note that tensile testing, a standard method for evaluating material properties, was not feasible for the MBC. Tensile tests are typically performed on thin rods or strips of material, which are subjected to tension until failure. However, due to the inherent characteristics of MBC, such as their inability to be cut or cultivated into thin strips or rods, conducting tensile tests was impossible.

2.1. Finite Element Method

Finite Element Method (FEM) stands as an indispensable tool for modeling and forecasting material responses within specific geometries. Its widespread application spans mechanical, civil, and aerospace engineering domains, simulating physical systems' behaviors under diverse environmental conditions.

The simulation work was conducted using the FEM software Abaqus/CAE 2021 developed by Dassault Systèmes SIMULIA [9]. Each model was meticulously crafted, incorporating geometries for composite base units and mycelium binding interfaces and supporting and load-bearing components through extruded section sketches. Material properties for both the mycelium and composite layers were defined within Abaqus, encompassing parameters such as density, Young's modulus, Poisson's ratio, and concrete plasticity damage values. These material properties were then assigned to relevant sections to specify their behavior within the FEM analysis. The composite material was modeled as a 3D deformable solid (C3D8R). At the same time, the mycelium was represented either as a deformable solid or a continuous, cohesive material (COH3D8), and any support or load-bearing components were treated as non-deformable rigid solids (R3D3, R3D4).

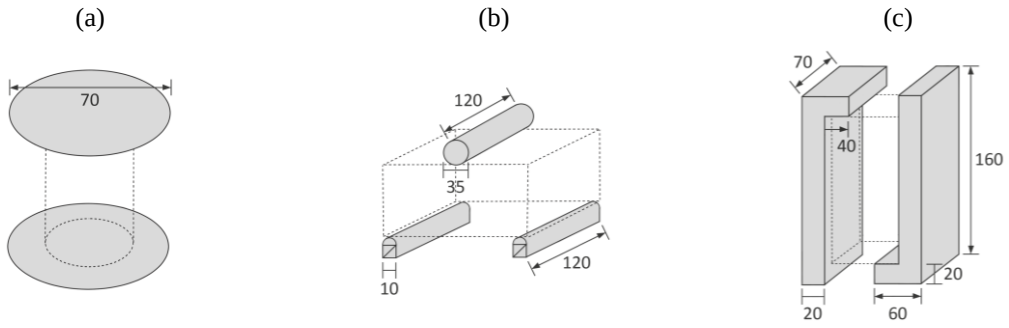

Figure 2: Part geometries for the support structures of (a) compression tests, (b) three-point bending tests, and (c) shear tests

The experimental setups were assembled by generating instances of individual parts and arranging them spatially to ensure direct surface contact. The support structure geometries utilized for the simulations are depicted in Figure 2. Abaqus' capability to automatically detect and assign contact pairs between surfaces separated by a specified distance was leveraged to establish contact interactions. A Kinematic "Hard" contact method with a friction coefficient 0.5 was employed between the specimen and the

support structures, while Tie Constraints were defined between the mycelium and composite layers. Detailed specifications of surfaces, contact pairs, and interactions are provided in the model code attachments for each test type.

Table 1: Field Output and History Output selection for all simulation models

	Field output
Interval	80
Stresses	S, Stress components and invariants; SVAG, Volume-averages stress components and invariants; MISES, Mises equivalent stress
Strains	PE, Plastic strain components; PEVAVG, Volume-averaged plastic strain components; PEEQ, Equivalent plastic strain; PEEQVAVG, Volume-averaged equivalent plastic strain; LE, Logarithmic strain components
Displacement	U, Translations and rotations; V, Translational and rotational velocities; A, Translational and rotational accelerations
Forces	RF, Reaction forces and moments
Contact	CSTRESS, Contact stresses
Failure	DAMAGEC, Compressive damage; DAMAGET, Tensile damage; DAMAGESHR, Shear damage
	History output (for whole model)
Frequency	n: 200
Energy	ALLEN, All energy totals
	History output (for the RP)
Frequency	n: 200
Displacement	U3, Translation (U2 for shear test)
Forces	RF3, Reaction force (RF2 for shear test)

Desired outputs for the models were selected, predominantly consisting of values summarized in Table 1. History Output was divided into two requests, one for the entire model and the other for a Reference Point on the support structure.

Furthermore, considering the dynamic nature of the simulations conducted in this study using the Dynamic Explicit calculation method, an amplitude was specified to allow for complex movement sequences. However, a simple linear movement from 0 to 1 was preferred in this case.

2.2. Previous Work on Anisotropic Simulation

Previous numerical modeling based on empirical test results was conducted at Trako using Abaqus/CAE software [10]. The different test setups are simulated according to their original geometry. The steel components were considered rigid bodies due to their stiffness relative to the test specimens and were connected with reference points. Specimens were uniformly displaced in the z-direction, and contact formulation was used to simulate support. Linear elements were used to mesh the specimens, with refinement at the specimen center for the bending test to simulate cracking accurately. A butterfly block mesh was applied for the compression test to ensure comparable element dimensions.

Different material models in Abaqus were investigated to represent the mycelium composite behavior, with separate definitions for bending and compressive loading due to the material's nonlinearities. A brittle cracking model was chosen for bending, a combined elastic-plastic model was used for compression, and the concrete-damaged plasticity model was used for shear. Material constants were derived from load-deformation curves, and optimization was performed for each parameter to approximate the curves adequately. The isotropic elasticity and general plasticity models were used to represent compressive behavior with Poisson's ratio assumption. Simulations revealed a lower Young's modulus under compression than bending, with an observed zone of increased compressive stress during elastic deformation. This led to expected cracking in the lateral edges due to transverse tensile stresses. Plastic deformation and associated damage processes were challenging to represent accurately. Still,

they could be effectively depicted by the chosen model, albeit with limitations in capturing the microscopic behaviors of the mycelium composite.

2.3. Isotropic Simulation

An isotropic simulation of the material was performed to reproduce the results produced by the method described in 2.2. Concrete Damage Plasticity was the chosen model for this simulation, as it is accurate and can be used for all three tests. The geometry of the test specimens can be found in Figure 3. Since Abaqus works dimensionless, the user must consistently enter all values. In this research, all lengths entered in Abaqus are equivalent to millimeters.

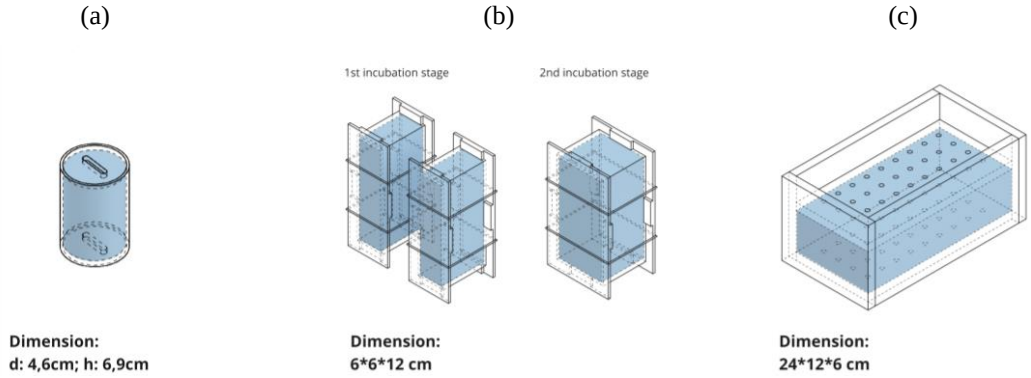

Figure 3: Geometry of simulated MBC in blue. The wireframe drawing represents the formwork to produce each test specimen: (a) Z1 cylinder, (b) VK cuboid, and (c) P2 cuboid

2.4. Material Classification

Data regarding European beech wood, scientifically known as *Fagus Sylvatica*, was gathered by V. Gryc et al. [11]. Information on pure mycelium was sourced from existing literature. Although Poisson's ratio for *G. Lucidum* hasn't been extensively studied, an estimation for pure mycelium can be derived using the rule of mixtures, as indicated in Formula 01, given the known values for the composite and beech wood [12].

$$\upsilon_M = \frac{(\upsilon_C - \upsilon_W \cdot V_W)}{V_M} \qquad \text{[Formula 01]}$$

The Poisson's ratios of the mycelium, beech wood, and composite material are denoted as vM, vW, and vC, respectively. VW and VM represent the volume fractions of the beech wood and the mycelium, respectively. The Poisson's ratio for *G. Lucidum* is then determined using the following calculation.

$$\upsilon_M = \frac{(0.14 - 0.32 \cdot 0.2062)}{V_M 0.7938} = 0.09 \qquad \text{[Formula 01]}$$

The MBC is considered a blend of beech wood and pure mycelium for this computation. However, this is merely an approximation since the beech wood undergoes changes and is consumed as a food source during mycelium growth. The resultant Poisson's ratio and collated material properties are recorded in Table 2.

Table 2: Mycelium, substrate, and MBC properties

	MBC [10]	***G. Lucidum*** [13]	***F. Sylbatica*** [11]
Density	2.9126E-10	1.34E-9	7.53E-10
Young's Modulus	8	26.8	2600
Poisson's Ratio	0.14	0.09	0.32

The Young's moduli for mycelium and MBC have been condensed into Figure 4, illustrated on an Ashby chart, a frequently used method for visually representing engineering material categories [14].

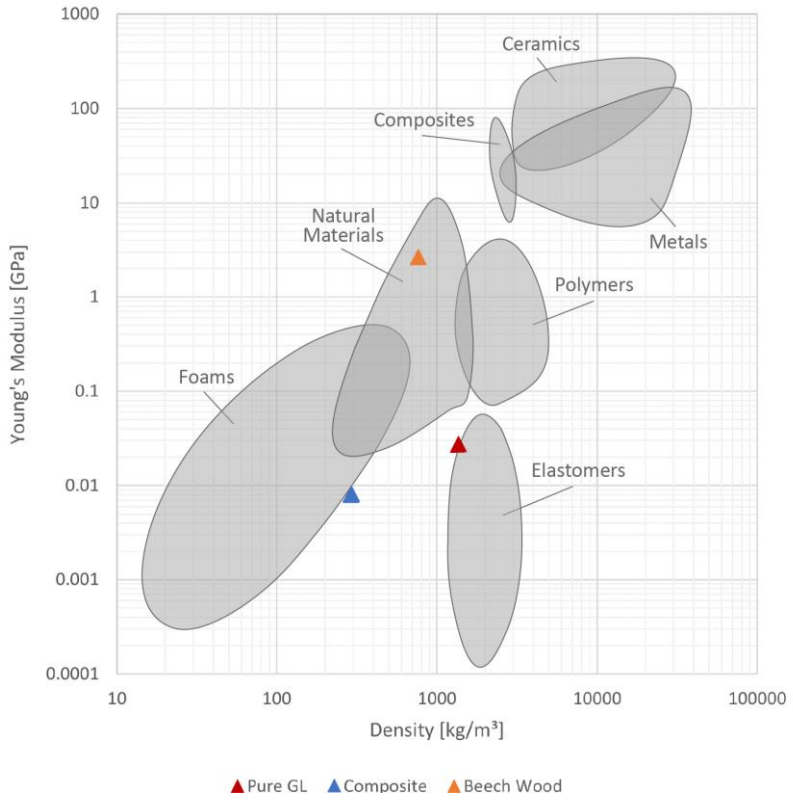

Figure 4: Visualization of MBC on an Ashby chart adapted by Gianna Hofman

Given that *G. Lucidum* is near elastomer regions, it might be presumed that its Poisson ratio would align closely with elastomers ($\nu = 0.50$). However, the computed value appears to be more akin to that of concrete ($0.10 \leq \nu \leq 0.20$) and foams ($0.10 \leq \nu \leq 0.40$), which is unexpected. This discrepancy could stem from the fact that Formula 01 is typically applied to materials with higher Young's moduli. Since mycelium represents a highly distinct material type that hasn't yet been fully explored, it's conceivable that it deviates from conventional engineering material norms. Consequently, without available literature values, a decision was made to proceed with $\nu = 0.09$ [15].

Beechwood, as depicted in Figure 4, is a natural material. When combined with the elastomer-like *G. Lucidum*, the resulting mycelium composite exhibits foam-like behavior, slightly beyond the recognized region for foam materials on the Ashby chart. The reduction in density and Young's modulus relative to the constituent materials likely arises from the composite's porosity.

3. Results and Discussion

3.1 Simulation of Compression Tests

As described in 2.1, non-cohesive compression tests were conducted utilizing FEM. As shown in Figure 5, stresses are concentrated in the mycelium binding interfaces, which causes the overall damage to be lower in composite base units or layers. Specifically, the stresses are highest towards the center of the specimen. The composite base units still show a slightly increased stress in the core, but this is significantly less than the introduced quasi-isotropic effect resulting from the binding-specific manufacturing process.

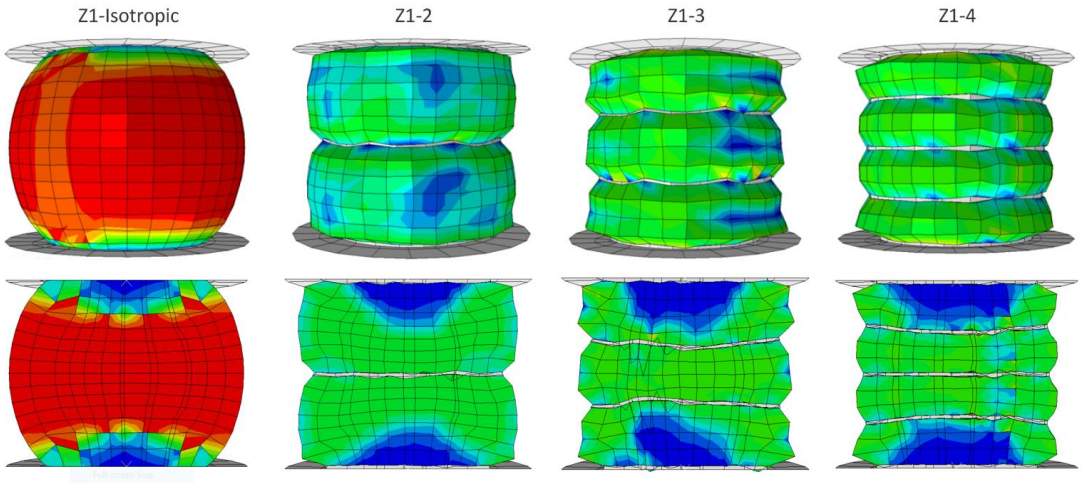

Figure 5: Simulation results for the Z1 using tie constraints showing the maximum compression damage of the composite base units in the cylinder's surface (top) and cross-section (bottom).

Figure 6 demonstrates that introducing mycelium interfaces induces an intense strain hardening behavior, as the reaction force increases with the displacement in the plastic deformation region.

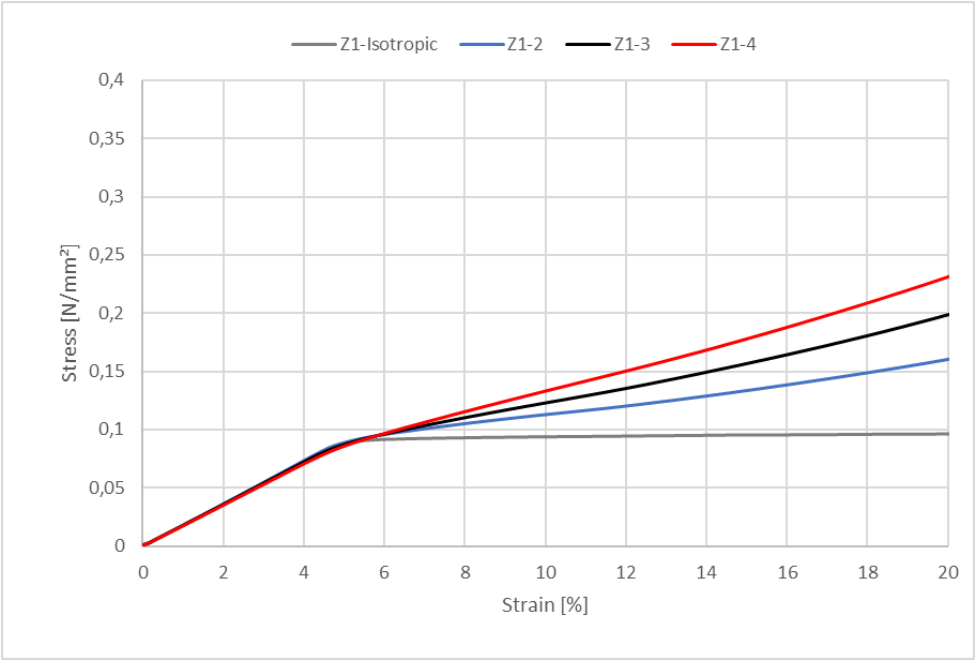

Figure 6: Stress-strain diagram of the compression simulation

3.2 Compression Tests

The compression behavior was investigated on cylindrical test specimens Z1-3 with a height of 6,9 cm and a diameter of 4,6 cm (Figure 7). Although previous research showed higher compression resistance on tests with a higher filling density [10], we decided to produce the test specimens with a tap density of 0.6 g/cm³ to prove if the binding-specific manufacturing process and its resulting lamination had a positive impact on them. After denaturation, the test specimens showed a dry density of 0.29 g/cm³. A total of twelve test specimens were produced. Three control test specimens were produced without a binding-specific manufacturing process (grey), and nine test specimens were made under a binding-specific manufacturing process with two (blue), three (black), and four (red) layers, respectively. The

tests were displacement-controlled with a test speed of 10mm/min. The force-deformation curves obtained from the tests were converted into stress-strain curves.

(a) (b) (c) (d)

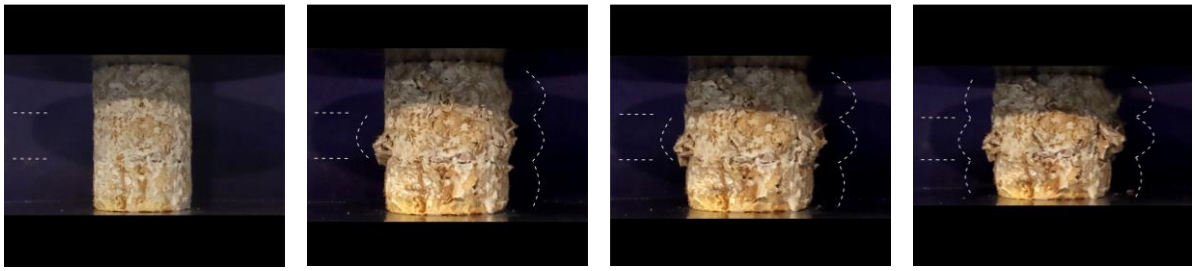

Figure 7: Compression tests of Z1-3 test specimens: (a) Z1-3 before loading; (b) Z1-3 after 1:27 min. loading; (c) Z1-3 after 1:46 min. loading; (d) Z1-3 after 2:00 min. loading

Figure 8 shows the stress-strain curves as results of the tests. In the control tests (grey curves), the stress-strain diagrams non-linear deformation behavior with a subsequent softening zone after slight consolidation. The maximum strength is compared at a strain value of 10%. In the case of the control tests, it amounts σ, max = 0.18 N/mm². Another series of test specimens with two layers -and one binding interface- was conducted (blue curves). The maximum strength of σ, max = 0.35 N/mm² is reached. Subsequently, three-layered -with two binding interfaces- test specimens were tested (black curves). Here, the maximum strength increased to σ, max = 0.40 N/mm². Finally, the four-layered test specimens -with three binding interfaces- were tested. The maximum strength increased to σ, max = 0.42 N/mm².

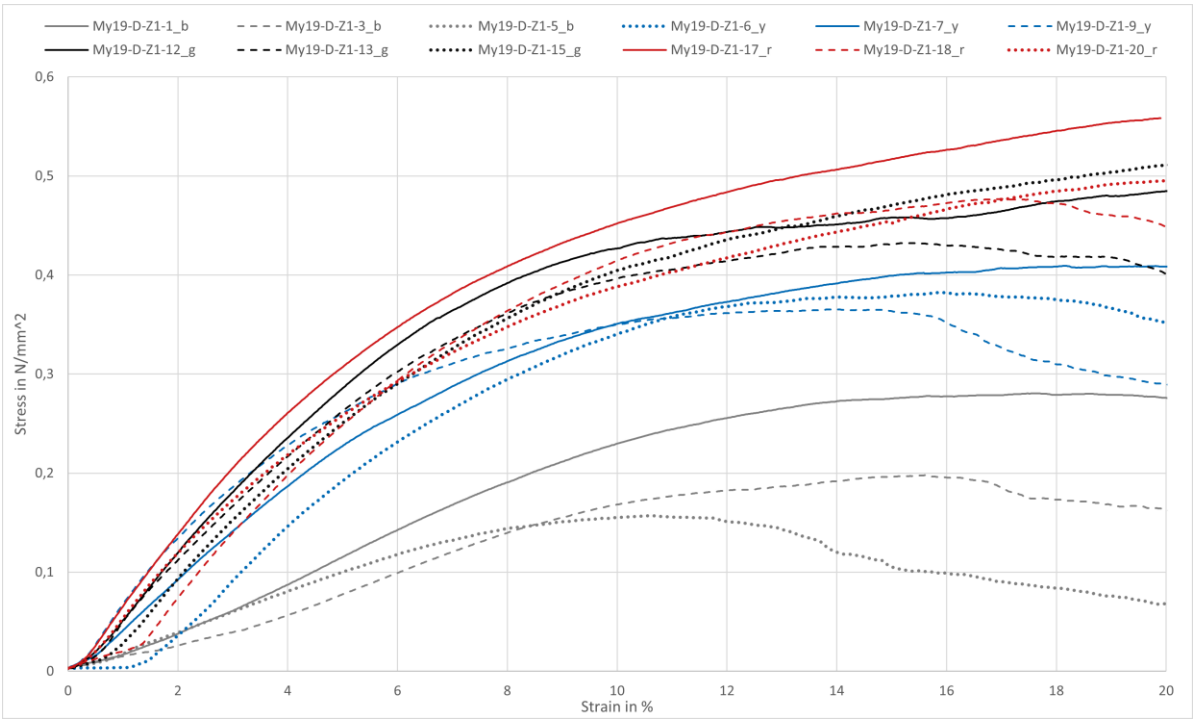

Figure 8: stress-strain curves of conducted compressive tests for each test specimen (grey: control tests, blue: two layers, black: three layers, and red: four layers)

Figure 9 shows the stress average influenced by the binding-specific manufacturing process, as we can observe. The compressive strength is twice as high for the layered test specimens as for the non-layered ones. Through the binding-specific manufacturing process, the specimen almost doubles the modulus of elasticity from 0.18 N/mm² to 0.42 N/mm². The results show the potential to improve structural

performance by increasing the number of layers or binding interfaces of quasi-pure mycelium, generating an anisotropic-like behavior.

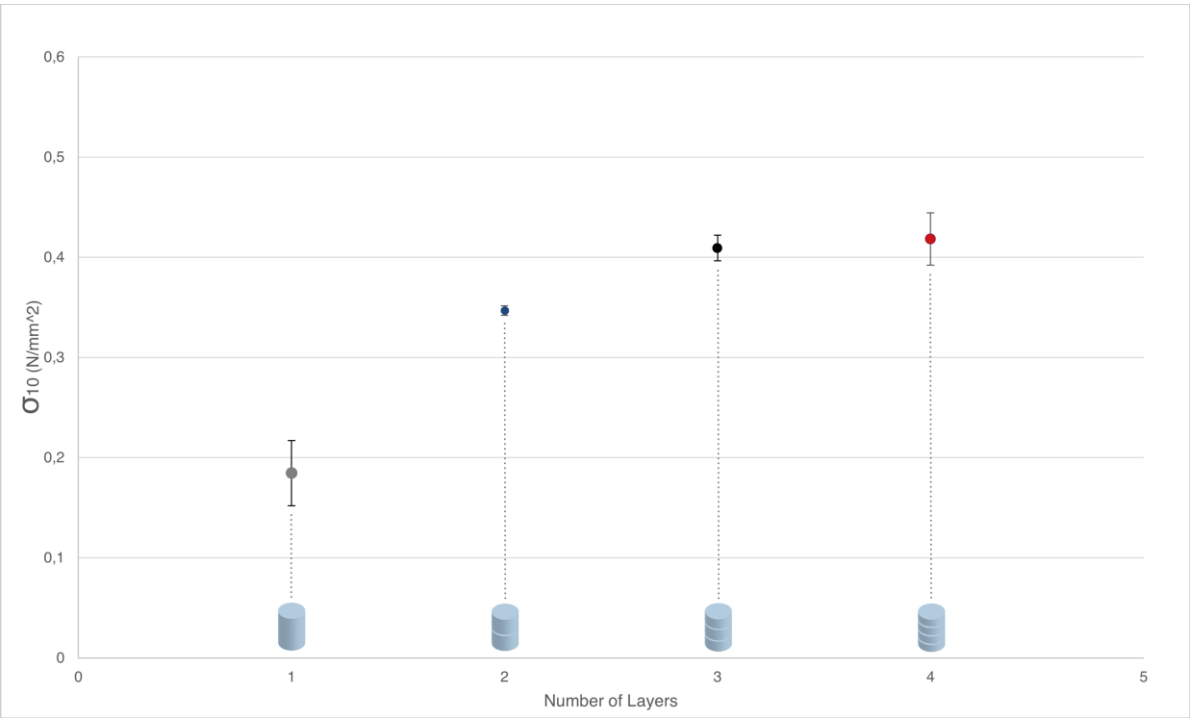

Figure 9: stress average influenced by the binding-specific manufacturing process: (1) control tests, (2) two-layered tests, (3) three-layered tests, and (4) four-layered tests

3.3 Simulation of Bending Tests

The results of the three-point bending test are shown in Figures 10 and 11, respectively. The maximum stresses are located in the mycelium interfaces, with the bottom ones absorbing more stress than the others. Compared to the isotropic case, the composite base units show very little stress, with only discernable stress directly underneath the load-inducing structure. Damage tends to cluster opposite where the force is applied, hinting at potential cracking or failure. In simulations with layered structures, multiple smaller crack-like damages are observed, contrasting with a single large crack seen in the uniform material [6].

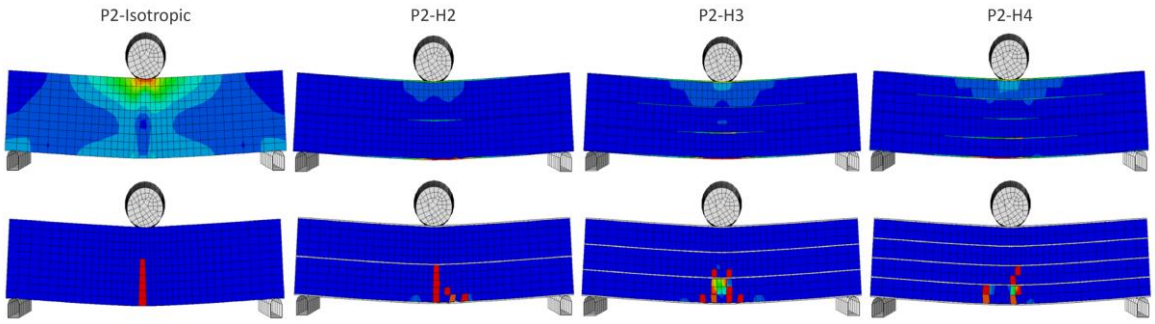

Figure 10: Simulation results in the cross-section of the P2 showing the maximum stresses in the specimen (top) and the maximum tensile damage of the composite interfaces (bottom).

When interpreting the reaction stress-strain curve for the P2 test specimens in Figure 11, material strength can be increased by introducing the mycelium interfaces. The bending modulus has risen significantly. Increasing mycelium binding interfaces does not seem to improve results, as the bending

modulus stays constant, and the maximum reaction force varies only lightly. The introduction of horizontally oriented mycelium interfaces between layers of the composite material significantly reduces the stresses faced by the composite. It thereby strengthens the overall specimen, but the failure behavior remains unchanged.

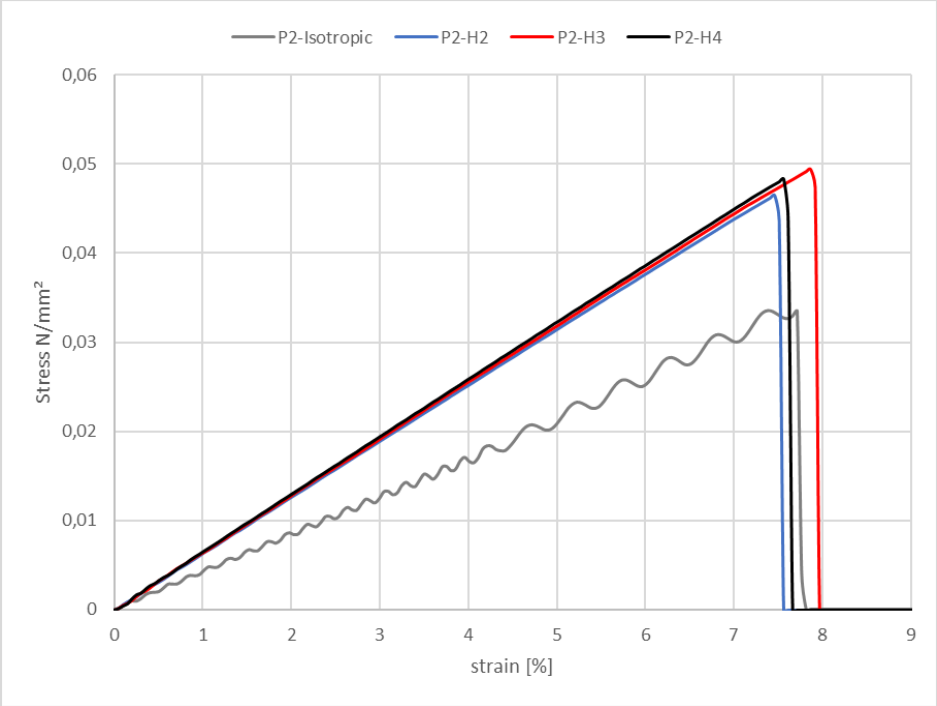

Figure 11: Stress-Strain curves of the binding simulation

3.4 Bending Tests

As shown in Figure 12, conducted bending tests characterize the material's behavior towards bending stresses. According to the standard DIN EN 12089:2013 specifications, specimens with the dimensions 24cm x 12cm x 6cm were produced and subjected to a three-point bending test (Figure 3, c).

(a) (b) (c) (d)

Figure 12: Bending tests of P1 test specimens: (a) P1 before loading; (b) P1 after 00:29 min. loading; (c) P1 after 00:31 min. loading; (d) P1 after 00:34 min. loading

Figure 13 depicts the stress-strain curves derived from the conducted tests. Across all tested specimens, a nearly linear elastic deformation range was observed until a strain of 4%, which was succeeded by a sudden failure indicative of the material's typical brittle fracture behavior. However, fracture manifestation occurs as a bending tensile fracture in the lower layer. This phenomenon arises from the

transition to ductile behavior in the binding area when the crack propagates, where the almost pure mycelium exhibits resistance, thus mitigating crack propagation.

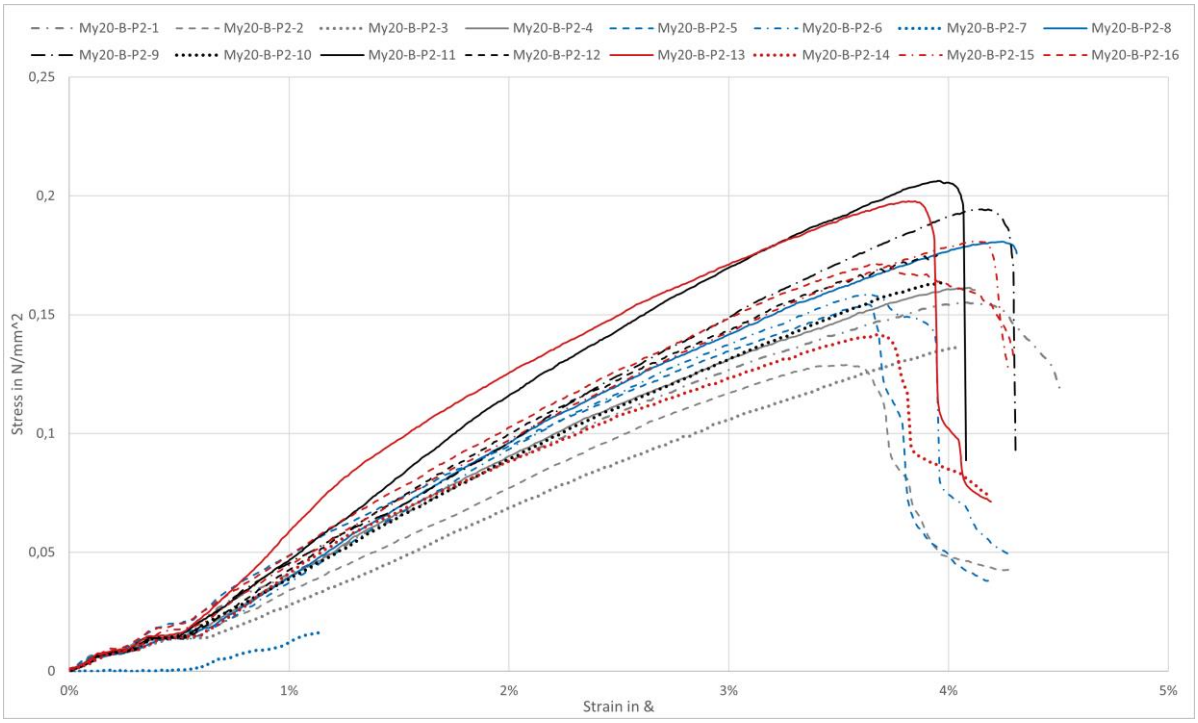

Figure 13: Stress-strain curves of the bending tests

Figure 14 shows the stress average influenced by the binding-specific manufacturing process. As we can observe, the resulting bending resistance is twice as high for the layered test specimens as for the non-layered ones. The specimen increases the bending resistance from 0.145 N/mm² to 0.185 N/mm² through the binding-specific manufacturing process. The results show the potential to improve structural performance by increasing the number of layers or binding interfaces of quasi-pure mycelium, generating an anisotropic-like behavior. It is essential to mention that MBC are less suitable to resist bending stresses [6], [7], [8].

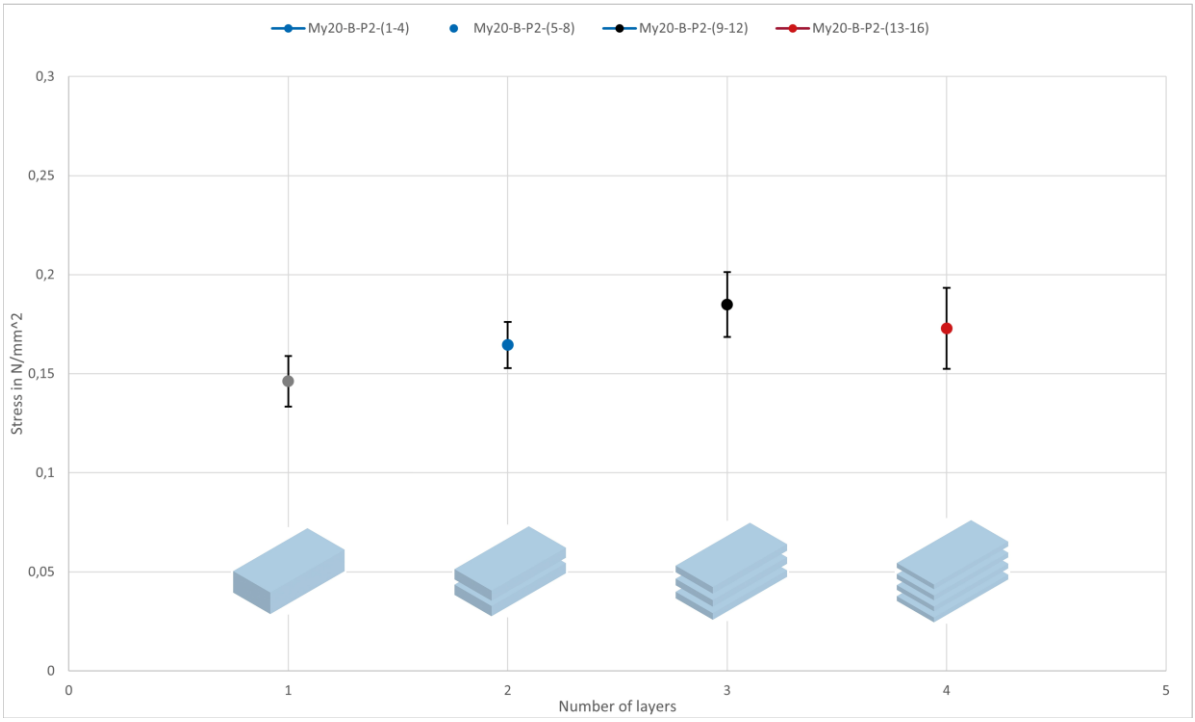

Figure 14: stress average influenced by the binding-specific manufacturing process: (1) control tests, (2) two-layered tests, (3) three-layered tests, and (4) four-layered tests

3.5 Simulation of Shear Tests

The results of the shear test simulations can be found in Figures 15 and 16. These figures show the stresses, compression damage, and reaction force over the displacement curve for the modeled VK test specimens, respectively.

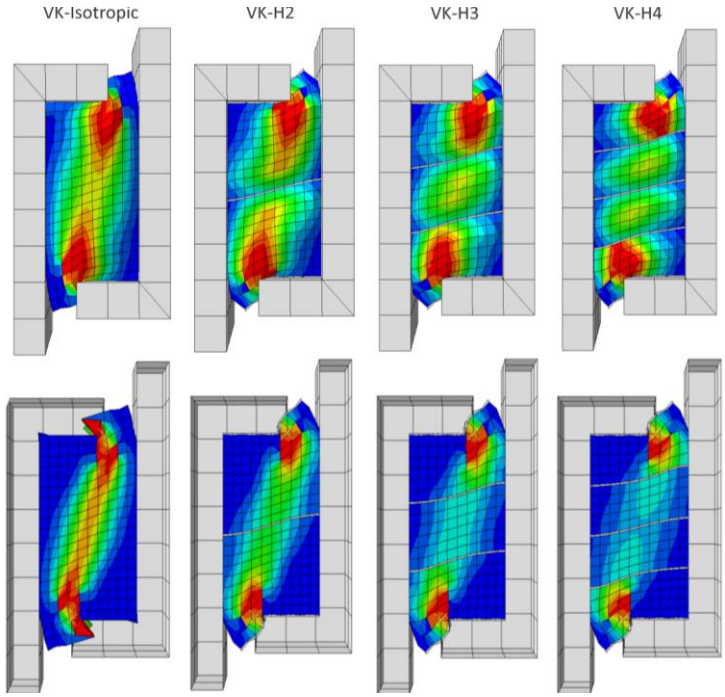

Figure 15: Results for the VK showing the maximum compression damage of the composite base units in the specimens surface (top) and cross-section (bottom)

Figure 16 shows that the compression damage follows the line between the two support frames, being the highest at the corners. In samples VK-3 and VK-4, the middle composite units face significantly less damage in the cross-section, which could be beneficial if applied as wall-building elements.

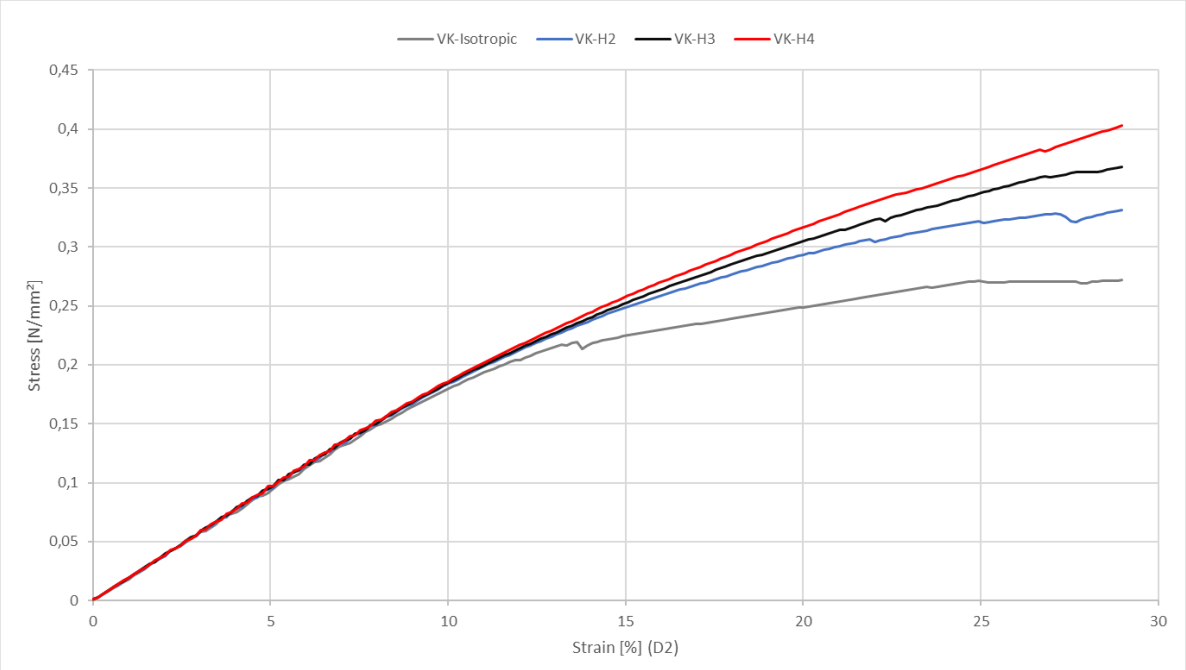

Figure 16: stress-strain curve of the shear simulations

Figure 16 shows the stress-strain curve with significant material hardening at high strains, increasing the effect with the number of mycelium binding interfaces. The addition of horizontal mycelium interfaces significantly improves the material's strength against shear forces.

3.6 Shear Tests

As shown in Figure 17, shear behavior was investigated through a simplified test setup in which the shear stress is introduced into the VK test specimens (6cm x 6cm x 12cm) by shearing the bearing surfaces (Figure 3, b).

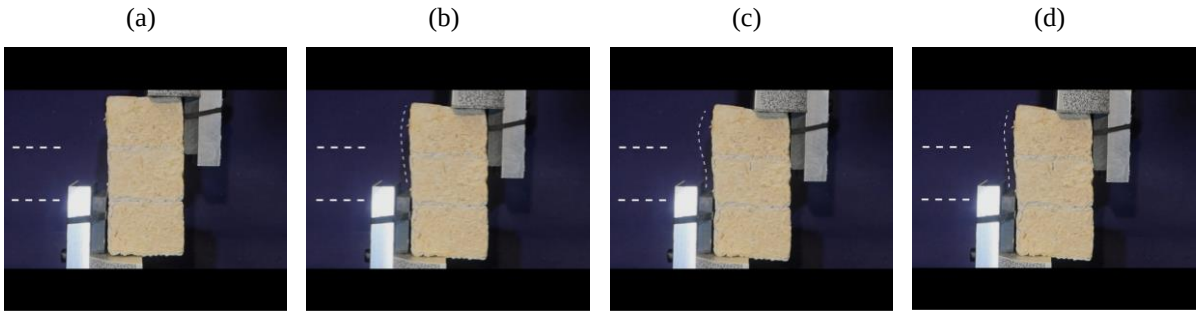

Figure 17: Shear tests of VK test specimens: (a) VK before loading; (b) VK after 11:55 min. Loading; (c) VK after 13:53 min. Loading; (d) VK after 16:01 min. loading

The strength experiences a near-linear increase in the initial two cases (VK-1 and VK-2) without a sudden decline, followed by a decrease in load-bearing capacity once the maximum value is attained. In

contrast, for most of the remaining test specimens (VK-3 and VK-4), the tests concluded upon reaching a strain of 10-12%, with no apparent failure or reduction in stress observed.

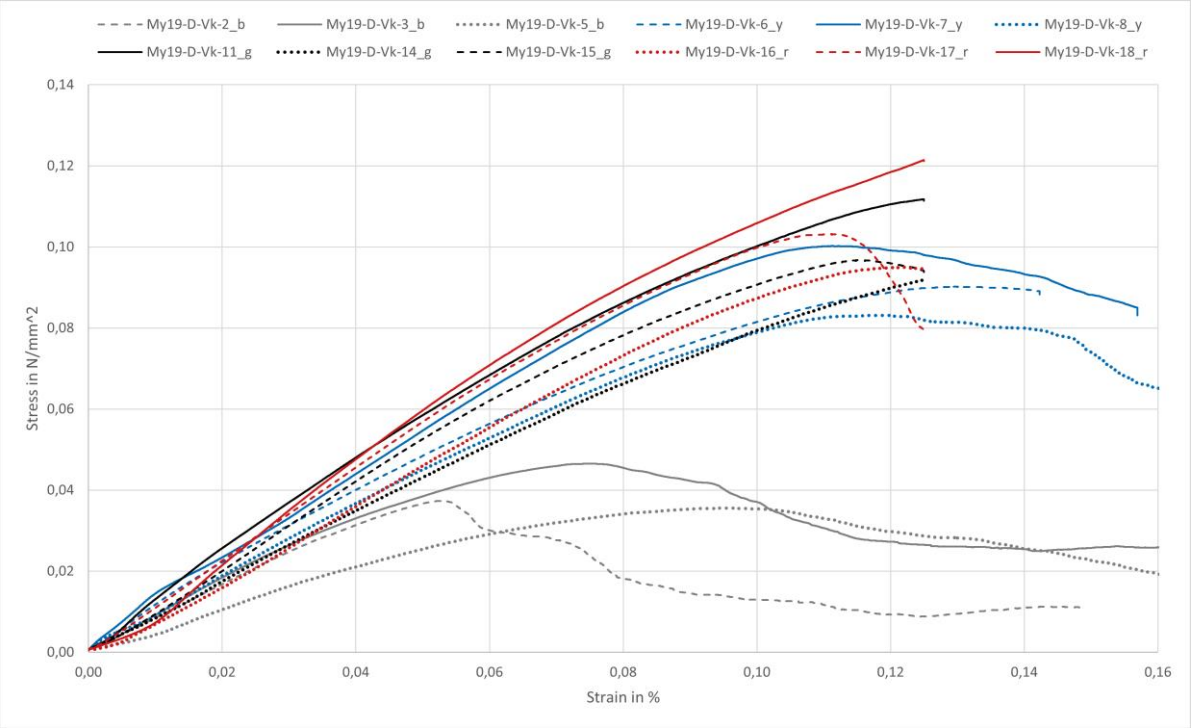

Figure 18: Stress-strain curves of the shear tests

Figure 19 shows the stress average influenced by the binding-specific manufacturing process, as we can observe. The shear strength is also twice as high for the layered test specimens as for the non-layered ones. Through the binding-specific manufacturing process, the specimen almost doubles the shear strength from 0.04 N/mm² to 0.1 N/mm². The results indicate that enhancing the structural performance can be achieved by increasing the number of binding interfaces in quasi-pure mycelium, resulting in a behavior similar to anisotropy. This suggests potential improvements of MBC in material design and engineering for better performance in structural applications.

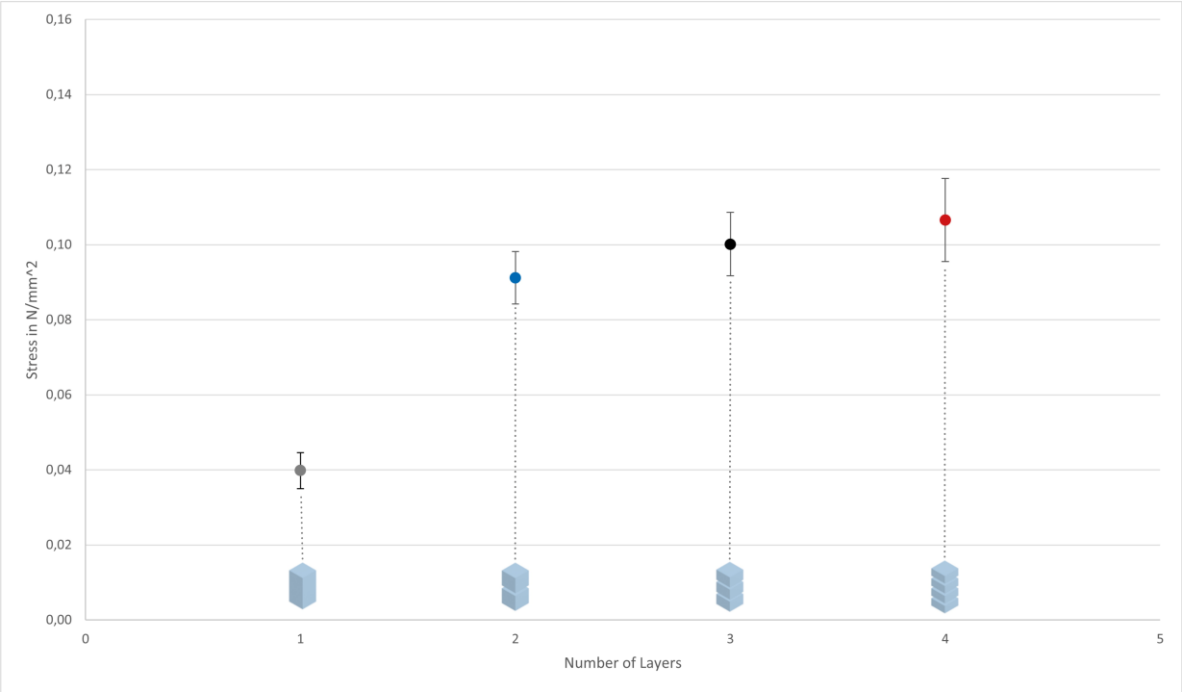

Figure 19: stress average influenced by the binding-specific manufacturing process: (1) control tests, (2) two-layered tests, (3) three-layered tests, and (4) four-layered tests

4. Conclusion and contribution

Usually, optimization efforts for MBC have focused on an isotropic approach, overlooking the potential advantages of anisotropic design through interface lamination. This research fills this gap by exploring the anisotropic behavior of MBC with binding interfaces, specifically assessing their impact on load-bearing elements constructed from multiple mycelium composite base units. This study sheds light on the directional dependencies induced by binding interfaces by investigating three engineered cases of anisotropy compared to standard isotropic test specimens.

In addition to exploring anisotropic design through biding interfaces, our study unveils crucial insights into the structural integrity of MBC. Specifically, we observe the phenomenon of mycelial growth into each other from both interfaces following the joining of test bodies, culminating in forming a seamless and homogeneous solid bond encasing the gap. Notably, within the maximum 1.0 mm thick gap, devoid of matrix particles (chips), the resultant bond exhibits a substantial increase in strength compared to the surrounding MBC material. Moreover, we observe a reinforcement of the mycelium in the interface area, characterized by enhanced strength and a higher degree of cross-linking. Our analysis reveals a positive correlation between interface area and strength, indicating the potential for tailored strength enhancements through deliberate interface manipulation.

One challenge in this research was the extended growth period required for a robust mycelial network, which delayed experiments by up to two months. To address this issue, a non-linear Finite Element Method (FEM) was proposed for numerical modeling. This approach allowed for the prediction of variations worth investigating and saved time by reducing the need for extensive empirical testing. The validity of the FEM simulations was confirmed through empirical tests, enabling controlled analysis of key variables such as compression, bending, and shear forces.

The observed improvements in strength properties can be attributed to the inherent characteristics of the mycelium structure. Specifically, the higher elastic proportion of chitin, constituting the scaffold structure of the mycelium, contributes significantly to the enhanced mechanical performance of the bonded interface. Furthermore, the absence of matrix particles within the gap further augments the structural integrity of the bond. Through this comprehensive understanding of the underlying mechanisms driving bond strength enhancement in MBC, our study expands the current knowledge base.

It offers practical insights for optimizing the design and fabrication of mycelium-based structural elements in construction applications.

Acknowledgments

All presented material tests were conducted at the Institute of Building Materials Research (ibac), RWTH Aachen. The research team extends their gratitude to student assistants at Trako Raman Suliman and Ulrich Spitel for their collaboration in our research efforts.

References

[1] German Federal Statistical Office (Destatis). *Waste balance 2020*, June 2022.

[2] M. Jones, A. Mautner, and S. Luenco et al. Engineered mycelium composite construction materials from fungal biorefineries: A critical review. *Materials and Design*, 187, December 2019.

[3] E. Elsacker, S. Vandelookb, and A. Van Wylicka et al. A Comprehensive Framework for the Production of Mycelium-based Lignocellulosic Composites. *Science of the Total Environment*, 725:138431, April 2020.

[4] D. Saez, D. Grizmann, M. Trautz, and A. Werner. Exploring the binding capacity of mycelium and wood-based 2 composites for use in construction. *Biomimetics*, 7(2), June 2021.

[5] D. Saez, D. Grizmann, A. Werner, and M. Trautz. Myzellbasierter Lignozellulose-Verbundswerkstoff, Patent DE 10 2021 134 036 A1, June 2023.

[6] D. Saez, D. Grizmann, M. Trautz, and A. Werner. Analyzing a fungal mycelium and chipped wood composite for use in construction. *In Proceedings of the IASS Symposium 2021*, Surrey, UK, August 2021.

[7] D. Saez, D. Grizmann, M. Trautz, and A.Werner. Developing sandwich panels with a mid-layer of fungal mycelium composite for a timber panel construction system. *In Proceedings of the World Conference on Timber Engineering 2021*, Santiago, Chile, September 2021.

[8] M. Trautz, D. Saez, D. Grizmann, and A.Werner. Myzelkomposit als vielseitig einsetzbarer, kreislaufgerechter Werkstoff für das Bauen. *NBau*, 2(2), July 2022.

[9] Dassault Systemes SIMULIA. ABAQUS/Standard User's Manual, Version 6.14. Dassault Systemes SIMULIA, 2014.

[10] U. Spittel. Numerical Model to Illustrate the Material Behavior of a Fungal Mycelium Composite. Bachelor Thesis at Chair of Structures and Structural Design, RWTH Aachen University, Aachen, Germany, April 2019. not publicly available.

[11] Š. Gomola V. Gryc, H. Vavrčík. Selected Properties of European Beech (Fagus sylvatica L.). *Journal of Forest Science*, 54(9):418–425, September 2008.

[12] D. Askeland, P. Fulay, and W. Wright, editors. *The Science and Engineering of Materials (6th edition)*. Cengage Learning, 2010.

[13] M. Antinori, M. Contardi, and G. Suarato et al. Advanced mycelium materials as potential self-growing biomedical scafolds. *Scientific Reports*, 11, June 2021.

[14] M. Ashby. Designing architectured materials. *Scripta Materialia*, *68*(1), January 2013.

[15] P. Mott and C. Roland. Limits to Poisson's ratio in isotropic materials. *Physical Review*, 80(132104), October 2009.